Inorg. Chem. **2007**, *46*, 4857−4867

Carbon−Fluorine Bond Cleavage in the Preparation of Osmium(III) and Osmium(IV) Fluorothiolate Complexes. Fluorine by Fluorine NMR-Assignment and Fluxional Processes

Maribel Arroyo,*,† Sylvain Bernès,‡ Margarita Cerón,† Verónica Cortina,† Consuelo Mendoza,† and Hugo Torrens§

Centro de Química del Instituto de Ciencias de la BUAP, Edificio 193 del Complejo de Ciencias, Ciudad Universitaria, San Manuel, 72570 Puebla, Puebla, Mexico, DEP, Facultad de Ciencias Químicas, UANL, Guerrero y Progreso S/N, Col. Treviño 64570, Monterrey, N.L., Mexico, and División de Estudios de Posgrado, Facultad de Química, UNAM, Ciudad Universitaria, 04510 México D.F., Mexico

Received October 13, 2006

Reactions of OsO_4 with HSR (R = C_6F_5, C_6F_4H-4,) in refluxing ethanol afford [Os(SC_6F_5)$_3$(SC_6F_4(SC_6F_5)-2)] (**1**) and [Os(SC_6F_4H-4)$_3$(SC_6F_3H-4-(SC_6F_4H-4)-2)] (**2**), which involve the rupture of C–F bonds. At room temperature, the compound [Os(SC_6F_5)$_3$(PMe_2Ph)$_2$] or [Os(SC_6F_5)$_4$(PMe_2Ph)] reacts with KOH(aq) in acetone, giving rise to [Os(SC_6F_5)(SC_6F_4(SC_6F_4O-2)-2)(PMe_2Ph)$_2$] (**3**), through a process involving the rupture of two C–F bonds, while the compound [Os(SC_6F_4H)$_4$(PPh_3)] reacts with KOH(aq) in acetone to afford [Os(SC_6F_4H-4)$_2$(SC_6F_3H-4-O-2)(PPh_3)] (**4**), which also implies a C–F bond cleavage. Single-crystal X-ray diffraction studies of **1**, **2**, and **4** indicate that these compounds include five-coordinated metal ions in essentially trigonal-bipyramidal geometries, whereas these studies on the paramagnetic compound **3** show a six-coordinated osmium center in a distorted octahedral geometry. ^{19}F, ^{1}H, $^{31}P\{^{1}H\}$, and COSY ^{19}F–^{19}F NMR studies for the diamagnetic **1**, **2**, and **4** compounds, including variable-temperature ^{19}F NMR experiments, showed that these molecules are fluxional. Some of the activation parameters for these dynamic processes have been determined.

Introduction

The chemical inertness and high thermal stability of fluorocarbons have made them useful in a variety of exceptional applications ranging from frying pan coating to artificial blood.[1] This chemical inertness makes the chemistry of fluorocarbons an area of research that has attracted the attention of inorganic and organometallic chemists, and new routes to transform these bonds are currently the subject of many investigations. The chemical and intellectual challenges of C−F bond activation rival those of C−H activation in hydrocarbons. Transition-metal compounds are employed as homogeneous catalysts to modify hydrocarbons in several industrial processes, such as olefin hydrogenations, hydroformylations, and polymerizations. Analogous processes do not presently exist for fluorocarbons, although it has become evident that interaction of fluorocarbons with metal centers may ultimately lead to the cleavage of the robust C−F bonds. The C−F bond activation of fluorinated hydrocarbons by transition-metal centers has been an area of intense study during the last years,[2−20] and catalytic systems have been

* To whom correspondence should be addressed. E-mail: slarroyo@siu.buap.mx.

† Centro de Química del Instituto de Ciencias de la BUAP, Edificio 193 del Complejo de Ciencias, Ciudad Universitaria.

‡ Facultad de Ciencias Químicas, UANL.

§ División de Estudios de Posgrado, Facultad de Química, UNAM, Ciudad Universitaria.

(1) (a) May, G. *Chem. Br.* **1997**, 34−36. (b) Clark, L. C.; Gollan, F. *Science* **1966**, *152* (3730), 1755−1756. (c) Wall, L. A. *Fluoropolymers*; Wiley-Interscience: New York, 1972; Vol. XXXV.

(2) Asplund, M. C.; Johnson, A. M.; Jakeman, J. A. *J. Phys. Chem. B* **2006**, *110* (1), 20−24.

(3) Maron, L.; Werkema, E. L.; Perrin, L.; Eisenstein, O.; Andersen, R. A. *J. Am. Chem. Soc.* **2005**, *127*, 279−292.

(4) Hughes, R. P.; Laritchev, R. B.; Zakharov, L. N.; Rheingold, A. L. *J. Am. Chem. Soc.* **2005**, *127*, 6325−6334.

(5) Burling, S.; Elliott, P. I. P.; Jasim, N. A.; Lindup, R. J.; Mckenna, J.; Perutz, R. N.; Archibald, S. J.; Whitwood, A. C. *J. Chem. Soc., Dalton Trans.* **2005**, 3686−3695.

(6) Piglosiewicz, I. M.; Kraft, S.; Beckhaus, R.; Haase, D.; Saak, W. *Eur. J. Inorg. Chem.* **2005**, 938−945.

(7) Villanueva, L.; Arroyo, M.; Bernès, S.; Torrens, H. *Chem. Commun.* **2004**, 1942−1943.

10.1021/ic0619660 CCC: $37.00
Published on Web 05/16/2007

developed.[21−23] The subject has been reviewed.[24−29]

Previously, we reported on the synthesis of $[Os(SR)_3(PMe_2Ph)_2]$ ($R = C_6F_4H$-4, C_6F_5).[30,31] The X-ray diffraction structure determination of the compound where $R = C_6F_5$[32] showed a C−F−Os interaction in the solid state. The interaction of an *o*-F of one of the SC_6F_5 ligands with the metal creates an S−F chelate ligand, resulting in six coordination in an approximately octahedral arrangement. We found that thermolysis of $[Os(SR)_3(PMe_2Ph)_2]$ in refluxing toluene causes a substantial rearrangement−oxidative reaction, giving a mixture of products that involves phosphine dissociation, cleavage of an *o*-C−F bond at a thiolate ligand, and transfer of a sulfur atom along with oxidation of the metal center.[32,33] We have now found that the formation of complexes **1**−**4** also involves the cleavage of C−F bonds.

Experimental Section

Materials and Methods. All reactions were carried out under argon using conventional Schlenk-tube techniques. Thin layer chromatography (Merck; 5−7.5 cm^2 Kiesegel 60 F_{254}) was used to monitor the progress of the reactions under study with hexanes−CH_2Cl_2 (4:1) as the eluent. The starting materials, thiols, phosphines, and osmium tetroxide, were from Aldrich Chemical Co. and used without further purification. Complexes $[Os(SC_6F_5)_3(PMe_2Ph)_2]$,[30,31] $[Os(SC_6F_5)_4(PMe_2Ph)]$,[34] and $[Os(SC_6F_4H)_4(PPh_3)]$[34] were prepared as published. The products were separated by passage through a silica gel chromatographic column with a hexanes−CH_2Cl_2 solution as the eluent.

Melting points were obtained on a Fisher-Johns melting point apparatus.

IR spectra were recorded over the 4000−400 cm^{-1} range on a Magna-Nicolet 750 Fourier transform IR spectrometer as KBr pellets. Data are expressed in wavenumbers (cm^{-1}) with relative intensities (vs = very strong, s = strong, m = medium, and w = weak).

^1H, ^{19}F, and COSY $^{19}F-^{19}F$ NMR spectra were recorded on a Varian Mercury VX400 spectrometer operating at 400 and 376 MHz, while $^{31}P\{^1H\}$ NMR spectra were recorded on a Varian Mercury VX300 spectrometer operating at 121 MHz. Chemical shifts are relative to tetramethylsilane [$\delta = 0$ (^1H)], CCl_3F [$\delta = 0$ (^{19}F)], and H_3PO_4 [$\delta = 0$ (^{31}P)] using $C_6D_5CD_3$ as the solvent.

The free energies of activation $\Delta G^{\ddagger}$ were calculated from variable-temperature (VT) ^{19}F NMR data using both the line-shape analysis and the Eyring equation for compounds **1** and **4**, and for each compound, both results are practically equal within experimental error. The line-shape analysis is not feasible for compound **2**, in which overlapping bands are present at several temperatures. Therefore, to have systematic results, all of the $\Delta G^{\ddagger}$ values reported in this paper have been calculated with the Eyring equation, estimating the rate constant at the coalescence temperature on the basis of the chemical shift difference at low temperature.

Positive-ion fast atom bombardment mass spectrometry (FAB^+-MS) spectra were recorded on a Jeol JMS-SX102A mass spectrometer operated at an accelerating voltage of 10 kV. Samples were desorbed from a 3-nitrobenzyl alcohol matrix using 3 keV xenon atoms. Mass measurements in FAB are performed at a resolution of 3000 using magnetic field scans and the matrix ions as the reference material.

Elemental analyses were determined by Galbraith Laboratories Inc.

Preparations. $[Os(SC_6F_5)_3(SC_6F_4(SC_6F_5)$-2)] (1). HSC_6F_5 (1.6 mL, 12 mmol) was dissolved in ethanol (60 mL), then OsO_4 (0.5 g, 2 mmol) was added, and the colorless mixture immediately turned black. The stirred mixture was refluxed for 3.5 h. After this time, the solvent was removed under vacuum, and the residue was purified by column chromatography (silica gel, hexane−CH_2Cl_2, 4.5:0.5). Compound **1** was obtained as green crystals (0.420 g, 18%) by slow evaporation of the eluent. Anal. Calcd for $C_{30}F_{24}OsS_5$: C, 30.88; S, 13.74. Found: C, 31.43; S, 13.65. Mp: 120 °C (dec). IR (KBr, cm^{-1}): 1506 (vs), 1488 (vs), 1462 (s), 1394 (w), 1092 (s), 1046 (w), 981 (vs), 854 (m). ^{19}F NMR ($C_6D_5CD_3$, −50 °C): δ ring **a**, δ −128.8 (dd, 1F, C_6F_4, $^3J_{F-F} = 23$ Hz, $^4J_{F-F} = 9$ Hz), −132.8 (m, 1F, C_6F_4), −142.7 (m, 1F, C_6F_4), −151.4 (t, 1F, C_6F_4, $^3J_{F-F} = 22$ Hz); ring **b**, δ −128.0 (d, 1F*o*, C_6F_5, $^3J_{Fo-Fm} = 19$ Hz), −135.2 (br s, 1F*o*, C_6F_5), −140.3 (t, 1F*p*, C_6F_5, $^3J_{Fp-Fm} = 22$ Hz), −155.4 (m, 1F*m*, C_6F_5), −156.9 (t, 1F*m*, C_6F_5, $^3J_{F-F} = 21$ Hz); ring **c**, δ −131.9 (d, 1F*o*, C_6F_5, $^3J_{Fo-Fm} = 23$ Hz), −132.2 (d, 1F*o*, C_6F_5, $^3J_{Fo-Fm} = 25$ Hz), −148.1 (t, 1F*p*, C_6F_5, $^3J_{Fp-Fm} = 21$ Hz), −160.2 (m, 1F*m*, C_6F_5), −160.8 (m, 1F*m*, C_6F_5); ring **d**, δ −130.7 (d, 1F*o*, C_6F_5, $^3J_{Fo-Fm} = 23$ Hz), −132.5 (d, 1F*o*, C_6F_5, $^3J_{Fo-Fm} = 25$ Hz), −148.6 (t, 1F*p*, C_6F_5, $^3J_{Fp-Fm} = 21$ Hz), −159.3 (m, 1F*m*,

(8) Clot, E.; Mégret, C.; Kraft, B. M.; Eisenstein, O.; Jones, W. D. *J. Am. Chem. Soc.* **2004**, *126*, 5647−5653.
(9) Bellabarba, R. M.; Nieuwenhuyzen, M.; Saunders, G. C. *Organometallics* **2003**, *22*, 1802−1810.
(10) Braun, T.; Rothfeld, S.; Schorlemer, V.; Stammler, A.; Stammler, H.-G. *Inorg. Chem. Commun.* **2003**, *6*, 752−755.
(11) Ferrando-Miguel, G.; Gérard, H.; Eisenstein, O.; Caulton, K. G. *Inorg. Chem.* **2002**, *41* (24), 6440−6449.
(12) Sladek, M. I.; Braun, T.; Neumann, B.; Stammler, H.-G. *J. Chem. Soc., Dalton Trans.* **2002**, 297−299.
(13) Kraft, B. M.; Jones, W. D. *J. Organomet. Chem.* **2002**, *658*, 132−140.
(14) Braun, T.; Cronin, L.; Higgitt, C. L.; McGrady, J. E.; Perutz, R. N.; Reinhold, M. *New J. Chem.* **2001**, *25* (1), 19−21.
(15) Barrio, P.; Castarlenas, R.; Esteruelas, M. A.; Lledós, A.; Maseras, F.; Oñate, E.; Tomàs, J. *Organometallics* **2001**, *20*, 442−452.
(16) Huang, D.; Koren, P. R.; Folting, K.; Davidson, E. R.; Caulton, K. G. *J. Am. Chem. Soc.* **2000**, *122*, 8916−8931.
(17) Whittlesey, M. K.; Perutz, R. N.; Moore, M. H. *Chem. Commun.* **1996**, 787−788.
(18) Hofmann, P.; Unfried, G. *Chem. Ber.* **1992**, *125*, 659−661.
(19) Crespo, M.; Martínez, M.; Sales, J. *J. Chem. Soc., Chem. Commun.* **1992**, 822−823.
(20) Blum, O.; Frolow, F.; Milstein, D. *J. Chem. Soc., Chem. Commun.* **1991**, 258−259.
(21) Aizenberg, M.; Milstein, D. *Science* **1994**, *265*, 359−361.
(22) Aizenberg, M.; Milstein, D. *J. Am. Chem. Soc.* **1995**, *117*, 8674−8675.
(23) Kuhl, S.; Schneider, R.; Fort, Y. *Adv. Synth. Catal.* **2003**, *345* (3), 341−344.
(24) Torrens, H. *Coord. Chem. Rev.* **2005**, *249*, 1957−1985.
(25) Richmond, T. G. *Angew. Chem., Int. Ed.* **2000**, *39*, 3241−3244.
(26) Richmond, T. G. In *Topics in Organometallic Chemistry*; Murai, S., Ed.; Springer: New York, 1999; Vol. 3, pp 243−269.
(27) Burdenuic, J.; Jedlicka, B.; Crabtree, R. H. *Chem. Ber.* **1997**, *130*, 145−154.
(28) Saunders, G. C. *Angew. Chem., Int. Ed. Engl.* **1996**, *35* (22), 2615−2617.
(29) Kiplinger, J. L.; Osterberg, C. E.; Richmond, T. G. *Chem. Rev.* **1994**, *94*, 373−411.
(30) Catalá, R. M.; Cruz-Garritz, D.; Hills, A.; Hughes, D. L.; Richards, R. L.; Sosa, P.; Torrens, H. *J. Chem. Soc., Chem. Commun.* **1987**, 261−262.
(31) Catalá, R. M.; Cruz-Garritz, D.; Sosa, P.; Terreros, P.; Torrens, H.; Hills, A.; Hughes, D. L.; Richards, R. L. *J. Organomet. Chem.* **1989**, *359*, 219−232.
(32) Arroyo, M.; Bernès, S.; Briansó, J. L.; Mayoral, E.; Richards, R. L.; Rius, J.; Torrens, H. *Inorg. Chem. Commun.* **1998**, *1*, 273−276.
(33) Arroyo, M.; Bernès, S.; Briansó, J. L.; Mayoral, E.; Richards, R. L.; Rius, J.; Torrens, H. *J. Organomet. Chem.* **2000**, *599*, 170−177.
(34) Arroyo, M.; Chamizo, J. A.; Hughes, D. L.; Richards, R. L.; Román, P.; Sosa, P.; Torrens, H. *J. Chem. Soc., Dalton Trans.* **1994**, 1819−1824.

Table 1. X-ray Parameters

complex	**1**	**2**	**3**	**4**
chem formula	$C_{30}F_{24}OsS_5 \cdot 0.5H_2O$	$C_{30}H_5F_{19}OsS_5$	$C_{34}H_{22}F_{13}OOsP_2S_3$	$C_{36}H_{18}F_{11}OOsPS_3$
fw	1175.81	1076.84	1041.84	992.85
space group	$P2_1/n$	$P2_1/c$	$P2_1/n$	$P2_1/c$
a/Å	14.8936(15)	18.3106(17)	8.416(2)	10.3807(11)
b/Å	16.227(2)	9.2362(11)	19.096(4)	22.029(3)
c/Å	15.9492(14)	20.0791(19)	22.572(4)	15.8319(17)
α/deg	90.00	90.00	90.00	90.00
β/deg	95.561(6)	97.707(8)	96.036(15)	100.694(9)
γ/deg	90.00	90.00	90.00	90.00
V/Å^3	3836.3(7)	3365.1(6)	3607.4(12)	3557.5(7)
Z	4	4	4	4
μ/mm^{-1}	3.739	4.230	3.894	3.894
R indices [$I > 2\sigma(I)$][a]	R1 = 4.23, wR2 = 10.39	R1 = 5.66, wR2 = 13.28	R1 = 3.70, wR2 = 6.63	R1 = 3.37, wR2 = 6.00%
R indices (all data)[a]	R1 = 6.19, wR2 = 11.51	R1 = 9.20, wR2 = 15.10	R1 = 6.87, wR2 = 7.52	R1 = 5.94, wR2 = 6.74
D_{calcd}/g·cm^{-3}	2.036	2.126	1.918	1.854
data/param	8767/557	8940/496	6335/491	6274/479
T/°C	25(1)	23(1)	21(1)	23(1)

[a] $R1 = (\sum||F_o| - |F_c||)/\sum|F_o|$; $wR2 = [(\sum w(F_o^2 - F_c^2)^2)/\sum w(F_o^2)^2]^{1/2}$.

C_6F_5), −159.8 (m, 1F*m*, C_6F_5); ring **e**, δ −131.3 (d, 2F*o*, C_6F_5, $^3J_{Fo-Fm} = 24$ Hz), −154.3 (t, 1F*p*, C_6F_5, $^3J_{Fp-Fm} = 21$ Hz), −162.0 (m, 2F*m*, C_6F_5). FAB$^+$-MS {*m/z* (%) [fragment]}: 1168 (62) [M$^+$], 969 (100) [M$^+$ − SC_6F_5], 802 (29) [M$^+$ − SC_6F_5 − C_6F_5], 770 (45) [M$^+$ − 2(SC_6F_5)], 603 (76) [M$^+$ − 2(SC_6F_5) − C_6F_5].

[Os(SC_6F_4H-4)$_3$(SC_6F_3H-4-(SC_6F_4H-4)-2)] (2). HSC_6F_4H-4 (1.6 mL, 12 mmol) was dissolved in ethanol (50 mL), and OsO_4 (0.5 g, 2 mmol) was added. The mixture rapidly turned black. The stirred mixture was refluxed for 3.5 h. After this time, a solid was filtered, which was washed with cold ethanol and hexane to give **2** as a microcrystalline green powder. An additional crop of **2** was recovered by column chromatography of the filtered solution (silica gel, hexanes−CH_2Cl_2, 4.5:0.5), and green crystals (0.450 g, 21%) were obtained by slow evaporation of the eluent. Anal. Calcd for $C_{30}H_5F_{19}OsS_5$: C, 33.46; H, 0.47; S, 14.89. Found: C, 33.54; H, 0.58; S, 15.48. Mp: 212 °C (dec). IR (KBr, cm^{-1}): 1494 (vs), 1374 (m), 1231 (m), 918 (s), 850 (m), 716 (m). ^{1}H NMR ($C_6D_5CD_3$, RT): δ 5.94 (tt, 1H, 1SC_6F_4H, $^3J_{Hp-Fm} = 9.6$ Hz, $^4J_{Hp-Fo} = 7.2$ Hz), 5.87 (tt, 1H, 1SC_6F_4H, $^3J_{Hp-Fm} = 9.6$ Hz, $^4J_{Hp-Fo} = 8.0$ Hz), 5.82 (tt, 1H, 1SC_6F_4H, $^3J_{Hp-Fm} = 9.6$ Hz, $^4J_{Hp-Fo} = 7.2$ Hz), 5.60 (tt, 1H, 1SC_6F_4H, $^3J_{Hp-Fm} = 9.6$ Hz, $^4J_{Hp-Fo} = 7.2$ Hz), 5.32 (m, 1H, *o*-OSC_6F_3H, $^3J_{Hp-Fm} = 9.6$ Hz, $^3J_{Hp-Fm} = 9.6$ Hz, $^4J_{Hp-Fo} = 7.3$ Hz). ^{19}F NMR ($C_6D_5CD_3$, −50 °C): ring **a**, δ −109.7 (m, 1F, C_6F_3H), −124.3 (dt, 1F, C_6F_3H, $^3J_{F-F} = 23$ Hz), −132.8 (m, 1F, C_6F_3H); ring **b**, δ −129.1 (m, 1F*o*, C_6F_4H), −134.1 (br m, 2F, C_6F_4H), −134.9 (m, 1F*m*, C_6F_4H); ring **c**, δ −131.4 (br s, 1F*o*, C_6F_4H), −132.7 (m, 1F*o*, C_6F_4H), −138.0 (m, 1F*m*, C_6F_4H, full integral = 2), −138.2 (m, 1F*m*, C_6F_4H); ring **d**, δ −130.8 (br s, 1F*o*, C_6F_4H), −133.1 (m, 1F*o*, C_6F_4H), −136.7 (m, 1F*m*, C_6F_4H), −138.0 (m, 1F*m*, C_6F_4H, full integral = 2); ring **e**, δ −131.0 (m, 2F*o*, C_6F_4H), −138.9 (m, 2F*m*, C_6F_4H). FAB$^+$-MS {*m/z* (%) [fragment]}: 1078 (19) [M$^+$], 897 (30) [M$^+$ − SC_6F_4H], 748 (8) [M$^+$ − SC_6F_4H − C_6F_4H], 716 (9) [M$^+$ − 2(SC_6F_4H)], 567 (18) [M$^+$ − 2(SC_6F_4H) − C_6F_4H].

[Os(SC_6F_5)(SC_6F_4(SC_6F_4O-2)-2)(PMe_2Ph)$_2$] (3). The purple complex [Os(SC_6F_5)$_3$(PMe_2Ph)$_2$] (0.2127 g, 0.2 mmol) was dissolved in acetone (15 mL). To this stirred solution was added 2 mL of an aqueous 0.20 M KOH solution. The mixture rapidly turned brown. The mixture was stirred at room temperature for 24 h, and its color turned dark blue. The solvent was removed under vacuum, and the residue was purified by column chromatography (silica gel, hexane−CH_2Cl_2, 3:2). Compound **3** was obtained as blue crystals (0.052 g, 25%) by slow evaporation of the eluent. Anal. Calcd for $C_{34}H_{22}F_{13}OOsP_2S_3$: C, 39.20; H, 2.13; S, 9.23. Found: 40.12; H, 2.26; S, 9.10. Mp: 234 °C. IR (KBr, cm^{-1}): 1509 (vs), 1493 (vs), 1470 (vs), 1086 (s), 973 (m), 944 (w), 912 (w), 853 (w), 746 (w). FAB$^+$-MS {*m/z* (%) [fragment]}: 1043 (48) [M$^+$], 905 (79) [M$^+$ − PMe_2Ph], 844 (80) [M$^+$ − SC_6F_5], 706 (8) [M$^+$ − SC_6F_5 − PMe_2Ph].

Compound **3** was also obtained in a similar yield by an analogous procedure from the green complex [Os(SC_6F_5)$_4$(PMe_2Ph)].

[Os(SC_6F_4H-4)$_2$(SC_6F_3H-4-(O-2))(PPh_3)] (4). The green complex [Os(SC_6F_4H-4)$_4$(PPh_3)] (0.2354 g, 0.2 mmol) was dissolved in acetone (15 mL). To this stirred solution was added 2 mL of an aqueous 0.20 M KOH solution. The mixture rapidly turned reddish brown. The mixture was stirred at room temperature for 36 h, and its color slowly changed to dark green. After this time, the solvent was distilled off under vacuum. The solid product was purified through a chromatographic column (silica gel, hexane−CH_2Cl_2, 4:1). Compound **4** was obtained as green crystals (0.024 g, 12%) by slow evaporation of the eluent. Anal. Calcd for $C_{36}H_{18}F_{11}OOsPS_3$: C, 43.55; H, 1.83; S, 9.69. Found: 42.71; H, 1.65; S, 9.28. Mp: 170 °C (dec). IR (KBr, cm^{-1}): 1491 (vs), 1470 (sh), 1372 (w), 1230 (m), 1176 (w), 916 (s), 847 (w), 712 (w). ^{1}H NMR ($C_6D_5CD_3$, RT): isomer A, δ 7.27 (m, 6.0H, PPh_3, full integral = 6.6), 6.67 (m, 9.0H, PPh_3, full integral = 9.9), 6.12 (m, 1H, *o*-OSC_6F_3H), 5.90 (br s, 2.0H, SC_6F_4H, full integral = 2.2); isomer B, δ 7.27 (m, 0.6H, PPh_3, full integral = 6.6), 6.67 (m, 0.9H, PPh_3, full integral = 9.9), 5.90 (br s, 0.2H, SC_6F_4H, full integral = 2.2), 5.62 (m, 0.1H, *o*-OSC_6F_3H). ^{19}F NMR ($C_6D_5CD_3$, RT): isomer A, thiolates, δ −134.0 (s, 4.0F*o*, SC_6F_4H, full integral = 4.4), −140.4 (br s, 2.0F*m*, SC_6F_4H, full integral = 2.2), −141.3 (br s, 2.0F*m*, SC_6F_4H, full integral = 2.2); isomer A, thiolate−phenoxide, δ −141.7 (m, 1F, *o*-OSC_6F_3H), −143.7 (m, 1F, *o*-OSC_6F_3H), −152.3 (ddd, 1F4, *o*-OSC_6F_3H, $^3J_{F4-F3} = 23$ Hz, $^4J_{F4-F6} = 10$ Hz, $^3J_{F4-H5} = 3$ Hz); isomer B, thiolates, δ −134.0 (s, 0.4F*o*, SC_6F_4H, full integral = 4.4), −140.4 (br s, 0.2F*m*, SC_6F_4H, full integral = 2.2), −141.3 (br s, 0.2F*m*, SC_6F_4H, full integral = 2.2); isomer B, thiolate−phenoxide, δ −118.3 (pt, 0.1F, *o*-OSC_6F_3H, $^4J_{F-F} = 11$ Hz), −138.0 (dd, 0.1F5, *o*-OSC_6F_3H, $^3J_{F5-F6} = 20$ Hz, $^3J_{F5-H4} = 10$ Hz), −170.2 (m, 0.1F, *o*-OSC_6F_3H). ^{31}P{^{1}H} NMR ($C_6D_5CD_3$, RT): isomer A, δ 3.1 (s, 1P, PPh_3); isomer B, δ 3.4 (s, 0.1P, PPh_3). FAB$^+$-MS {*m/z* (%) [fragment]}: 994 (94) [M$^+$], 917 (5) [M$^+$ − Ph], 813 (10) [M$^+$ − SC_6F_4H], 663 (18) [M$^+$ − SC_6F_4H − C_6F_4H − H], 631 (5) [M$^+$ − SC_6F_4H − C_6F_4H − H − S].

X-ray Diffraction Data. Air-stable single crystals of complexes **1**−**4** were obtained by slow evaporation of solutions as described above. Pertinent crystal data and other crystallographic parameters are listed in Table 1. Diffraction data were collected at 294−298 K on a Bruker P4 diffractometer using graphite-monochromated Mo Kα radiation ($\lambda = 0.710\,73$ Å) and standard procedures.[35]

Table 2. Selected Bond Lengths (Å) and Angles (deg) for **1**

Os1−S2	2.1976(15)	Os1−S3	2.2034(15)	Os1−S4	2.2343(15)
Os1−S1	2.3739(13)	Os1−S5	2.4020(14)	S1−C1	1.778(6)
S1−C7	1.773(6)	S2−C12	1.786(6)	S3−C13	1.764(5)
S4−C19	1.766(6)	S5−C25	1.769(6)		
S2−Os1−S3	118.73(6)	S2−Os1−S4	125.14(6)	Os1−S1−C1	114.21(19)
S3−Os1−S4	116.11(6)	S2−Os1−S1	88.30(5)	Os1−S1−C7	103.83(19)
S3−Os1−S1	94.96(5)	S4−Os1−S1	88.75(5)	Os1−S2−C12	106.8(2)
S2−Os1−S5	85.66(6)	S3−Os1−S5	89.71(5)	Os1−S3−C13	111.44(18)
S4−Os1−S5	93.08(5)	S1−Os1−S5	173.64(5)	Os1−S4−C19	110.48(19)
				Os1−S5−C25	109.83(18)

Table 3. Selected Bond Lengths (Å) and Angles (deg) for **2**

Os1−S2	2.1965(17)	Os1−S3	2.2139(19)	Os1−S4	2.2186(18)
Os1−S1	2.3829(16)	Os1−S5	2.401(2)	S1−C1	1.779(6)
S1−C7	1.773(7)	S2−C12	1.767(7)	S3−C13	1.791(8)
S4−C19	1.779(7)	S5−C25	1.752(8)		
S2−Os1−S3	118.00(8)	S2−Os1−S4	121.61(7)	Os1−S1−C1	113.7(2)
S3−Os1−S4	120.38(8)	S2−Os1−S1	88.43(6)	Os1−S1−C7	103.2(2)
S3−Os1−S1	94.95(7)	S4−Os1−S1	87.82(6)	Os1−S2−C12	106.8(2)
S2−Os1−S5	91.31(7)	S3−Os1−S5	83.23(8)	Os1−S3−C13	109.7(3)
S4−Os1−S5	94.19(7)	S1−Os1−S5	177.79(7)	Os1−S4−C19	112.8(2)
				Os1−S5−C25	109.2(3)

Table 4. Selected Bond Lengths (Å) and Angles (deg) for **3**

Os1−O42	2.099(4)	Os1−S3	2.3247(16)	S3−C31	1.762(6)
Os1−P2	2.3414(16)	Os1−P1	2.3559(17)	S4−C36	1.799(6)
Os1−S5	2.3659(16)	Os1−S4	2.4035(15)	S4−C41	1.795(6)
				S5−C51	1.771(6)
O42−Os1−S3	90.70(12)	O42−Os1−P2	85.77(12)	Os1−S3−C31	105.4(2)
S3−Os1−P2	92.82(6)	O42−Os1−P1	178.21(13)	Os1−S4−C36	103.24(19)
S3−Os1−P1	87.57(6)	P2−Os1−P1	94.74(6)	Os1−S4−C41	97.3(2)
O42−Os1−S5	93.26(12)	S3−Os1−S5	175.96(6)	Os1−S5−C51	109.2(2)
P2−Os1−S5	88.26(6)	P1−Os1−S5	88.46(6)		
O42−Os1−S4	82.43(11)	S3−Os1−S4	87.34(5)		
P2−Os1−S4	168.20(6)	P1−Os1−S4	97.05(6)		
S5−Os1−S4	92.40(5)				

Table 5. Selected Bond Lengths (Å) and Angles (deg) for **4**

Os1−O20	2.084(3)	Os1−S1	2.1909(13)	S1−C19	1.758(5)
Os1−S3	2.2132(15)	Os1−S2	2.2213(14)	S2−C25	1.794(5)
Os−P1	2.3333(12)			S3−C31	1.791(5)
O20−Os1−S1	85.11(9)	O20−Os1−S3	92.44(11)	Os1−S1−C19	101.25(18)
S1−Os1−S3	118.16(6)	O20−Os1−S2	89.88(10)	Os1−S2−C25	107.22(18)
S1−Os1−S2	120.36(6)	S3−Os1−S2	121.42(6)	Os1−S3−C31	108.06(19)
O20−Os1−P1	176.54(9)	S1−Os1−P1	91.43(4)		
S3−Os1−P1	89.31(5)	S2−Os1−P1	91.76(5)		

Structures were solved and refined[36] on the basis of absorption-corrected data (ψ scans). Structures were refined without restraints or constraints for non-hydrogen atoms. Hydrogen atoms were placed in idealized positions and refined using a riding approximation with constrained bond lengths and fixed isotropic displacement parameters. In the case of **1**, disordered water molecules were found in the crystal structure, probably arising from ethanol used as the solvent for the synthesis. However, it is unclear why water was included in the case of **1** and not for other complexes. One molecule (O1) lies in a general position, while the other (O2) lies on an inversion center. Site occupation factors were first roughly refined and eventually fixed to $^1/_4$ in the last refinement cycles. Complete crystallographic data were deposited in CIF format. Structure factors are available upon request to the authors.

Selected geometric parameters for **1**−**4** are listed in Tables 2−5, respectively.

(35) *XSCAnS Users Manual*, release 2.21; Siemens Analytical X-ray Instruments Inc.: Madison, WI, 1996.
(36) Sheldrick, G. M. *SHELXTL-plus*, release 5.10; Siemens Analytical X-ray Instruments Inc.: Madison, WI, 1998.

Results and Discussion

We have previously reported the C−F bond cleavage, by thermolysis reactions in refluxing toluene, of the osmium(III) compounds $[Os(SR)_3(PMe_2Ph)_2]$ (R = C_6F_4H-4 or C_6F_5). We have now found related C−F bond ruptures during the formation of the osmium(IV) compounds **1** and **2** from OsO_4 and an excess of HSR in refluxing ethanol. As discussed below, the reaction products have been identified according to Schemes 1 and 2.

On the other hand, the room-temperature reaction between the osmium(III) compound $[Os(SC_6F_5)_3(PMe_2Ph)_2]$ in acetone and an aqueous solution of KOH gives rise to **3**, the formation of which requires the cleavage of two C−F bonds. Compound **3** is also obtained by the analogous reaction with the osmium(IV) compound $[Os(SC_6F_5)_4(PMe_2Ph)]$, as shown in Scheme 3.

However, the room-temperature reaction of the osmium(IV) compound $[Os(SC_6F_4H)_4(PPh_3)]$ in acetone with

Scheme 1

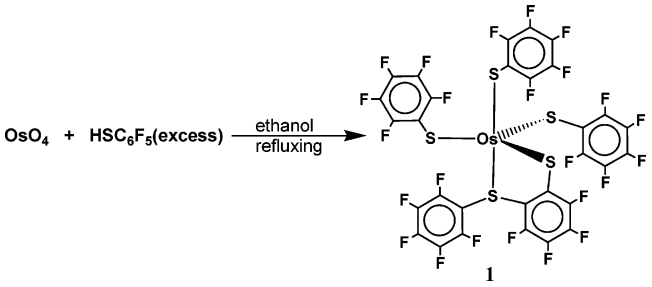

Scheme 2

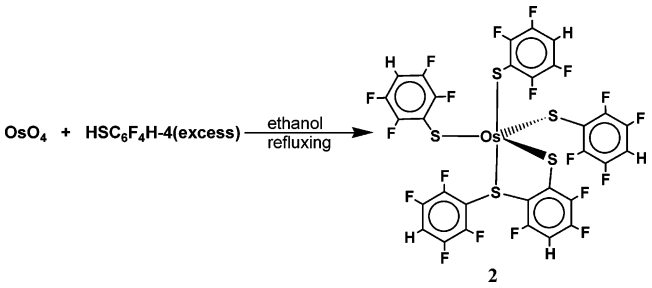

an aqueous solution of KOH gives rise to **4**, the formation of which also requires the cleavage of a C−F bond (Scheme 4).

Complexes **1**−**4** were isolated by column chromatography as crystalline and air-stable solids. These osmium(IV) (**1**, **2**, and **4**) and osmium(III) (**3**) compounds were characterized by elemental analyses, FAB^+-MS spectrometry, and spectroscopy. The FAB-MS spectra of compounds **1** and **2** show the corresponding parent ions (**1**, m/z = 1168, 62%; **2**, m/z = 1078, 19%) from which successive losses of two SC_6F_5 (or SC_6F_4H) and one C_6F_5 (or C_6F_4H) (**1**, m/z = 969, 100%, m/z = 770, 45%, m/z = 603, 76%; **2**, m/z = 897, 30%, m/z = 716, 9%, m/z = 567, 18%) are observed. The loss of C_6F_5 (or C_6F_4H) from the ion $[Os(SC_6F_5)_2(SC_6F_4(SC_6F_5)\text{-}2)]^+$ (or $[Os(SC_6F_4H)_2(SC_6F_3H(SC_6F_4H)\text{-}2)]^+$) is also observed (**1**, m/z = 802, 29%; **2**, m/z = 748, 8%). The C−F bond cleavage in the formation of **1** and **2** is confirmed by X-ray structure determinations, which are shown in Figures 1 and 2, respectively.

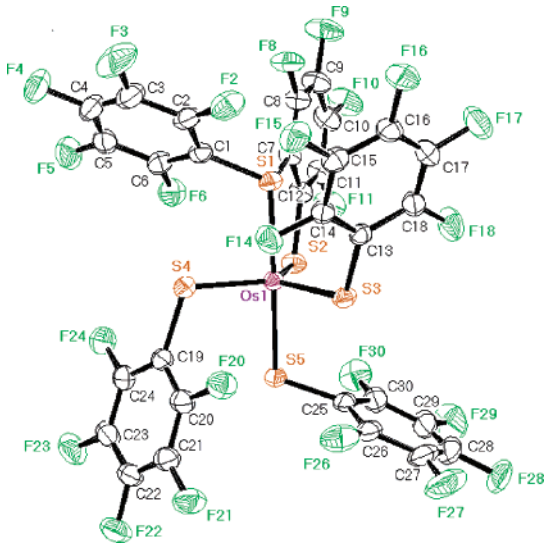

Figure 1. Structure of **1** showing thermal displacement parameters at the 30% probability level. Water is omitted for clarity.

The FAB-MS spectrum of complex **3** shows the parent ion (m/z = 1043, 48%) from which losses of PMe_2Ph and SC_6F_5 (m/z = 905, 79%, m/z = 844, 80%) are observed. The subsequent losses of SC_6F_5 or PMe_2Ph, respectively, give rise to the ion $[Os(SC_6F_4(SC_6F_4O)\text{-}2)(PMe_2Ph)]^+$ (m/z = 706, 8%). The paramagnetism of this d^5 osmium(III) compound precluded structural NMR studies in solution, but fortunately single crystals of **3** were obtained and its X-ray structure is shown in Figure 3, from which it is evident that the formation of compound **3** implies the rupture of two C−F bonds from the original C_6F_5 rings belonging to the starting material, in addition to the incorporation of an oxygen atom and the formation of a C−S bond.

The FAB-MS spectrum of complex **4** shows the parent ion (m/z = 994, 92%) from which successive losses of SC_6F_4H, $C_6H_2F_4$, and S (m/z = 813, 10%, m/z = 663, 18%, m/z = 631, 5%) are observed. The C−F bond cleavage in the formation of **4** is also confirmed by the X-ray structure, which is shown in Figure 4.

The X-ray-characterized complexes are mononuclear species: three of them (**1**, **2**, and **4**) with five-coordinated metal

Scheme 3

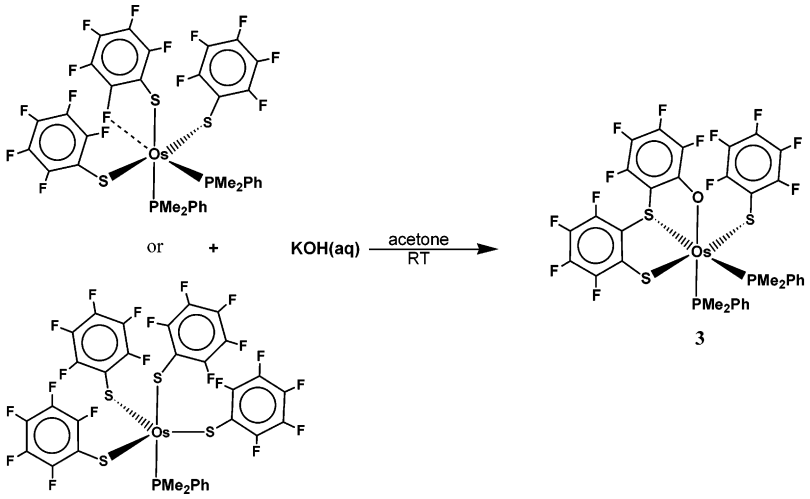

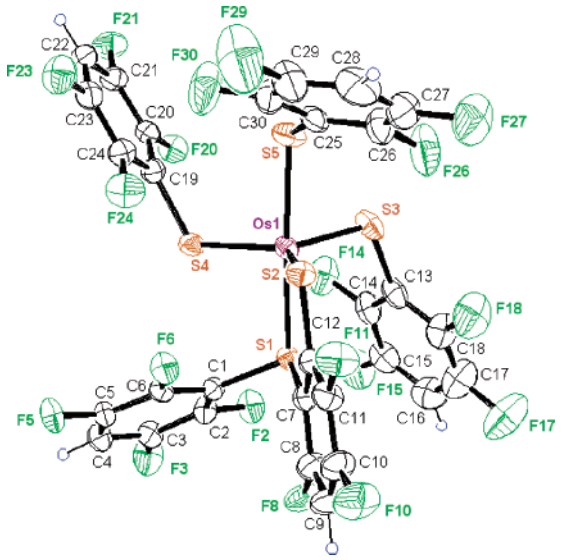

Figure 2. Structure of **2** showing thermal displacement parameters at the 30% probability level for non-hydrogen atoms. Hydrogen atom labels are omitted for clarity.

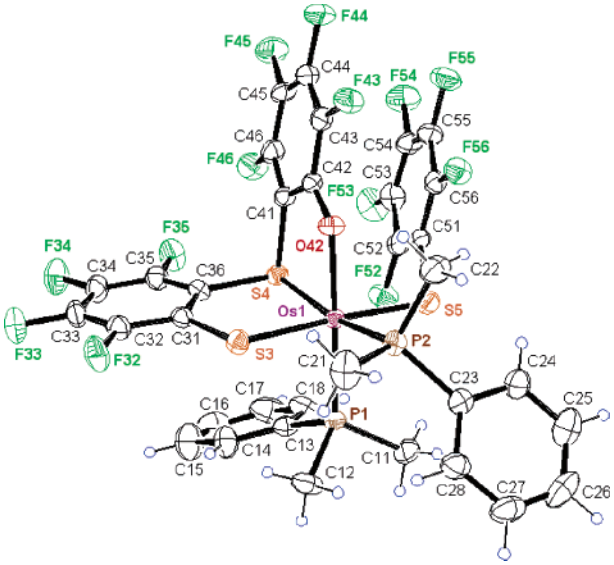

Figure 3. Structure of **3** showing thermal displacement parameters at the 30% probability level for non-hydrogen atoms. Hydrogen atom labels are omitted for clarity.

Scheme 4

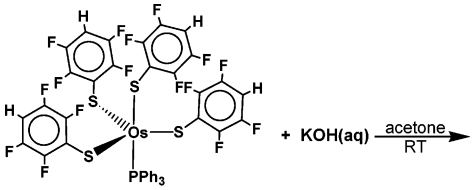

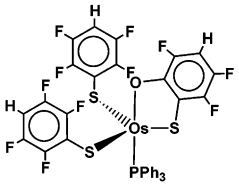

4

ions in essentially trigonal-bipyramidal geometry, whereas compound **3** has a six-coordinated metal center in a distorted octahedral geometry.

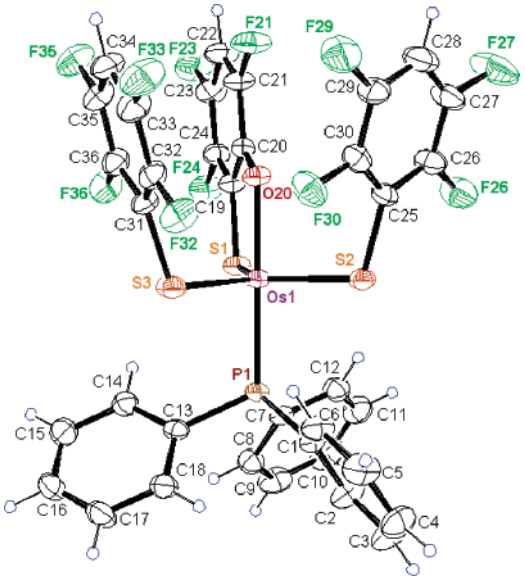

Figure 4. Structure of **4** showing thermal displacement parameters at the 30% probability level for non-hydrogen atoms. Hydrogen atom labels are omitted for clarity.

The structures of **1** and **2** consist of discrete essentially trigonal-bipyramidal molecules with a persulfurated coordination sphere. These two structures show the same arrangement and conformation of the ligands. Two of the three equatorial positions are occupied by thiolate ligands ($SC_6F_5^-$, **1**, or $SC_6F_4H^-$, **2**) oriented trans with respect to the trigonal plane, "one-up, one-down". The third thiolate ligand ($SC_6F_5^-$, **1**, or $SC_6F_4H^-$, **2**) is coordinated in an axial position. The chelating thiolate−thioether ligand [$(SC_6F_4(SC_6F_5))^-$, **1**, or $(SC_6F_3H(SC_6F_4H))^-$, **2**] occupies an axial position [through S1 (thioether)] and an equatorial one [through S2 (thiolate)]. This arrangement is analogous to that observed in the related complex [Ru(SC_6HMe_4-2,3,5,6)$_3$($SCHMeCH_2SC_6HMe_4$-2,3,5,6)].[37] For obvious steric reasons, the pentafluorophenyl **1** or tetrafluorophenyl **2** ring at S1*ax* is staggered with respect to the S2−Os1−S4 angle (dihedral angle between phenyl and Os1/S2/S4 planes: 42.30(2)° in **1** and 37.5(2)° in **2**, corresponding to a gauche conformation). As a consequence, the S2−Os1−S4 angle is the largest of the three S*eq*−Os−S*eq* angles in each of these molecules. As might be expected,[38] the axial Os−$S_{thiolate}$ bond length [2.4020(14) Å for **1** or 2.401(2) Å for **2**] is longer than the equatorial Os−$S_{thiolate}$ bond lengths [2.1976(15)−2.2343(15) Å for **1** or 2.1965(17)−2.2186(18) Å for **2**]. The axial Os−$S_{thioether}$ distance [2.3739(13) Å for **1** or 2.3829(16) Å for **2**] is slightly shorter than the axial Os−$S_{thiolate}$ distance.

The X-ray diffraction study of **3** reveals a distorted octahedral geometry around the osmium center with a thiolate−thioether−phenoxide ligand, $(SC_6F_4(SC_6F_4O\text{-}2)\text{-}2)^{2-}$, where the $S3_{thiolate}$, $S4_{thioether}$, and $O42_{phenoxide}$ atoms occupy three facial positions. A PMe_2Ph ligand is coordinated trans to the $O42_{phenoxide}$ atom, and a second PMe_2Ph ligand is trans to the $S4_{thioether}$ atom. The coordination sphere is completed by a $SC_6F_5^-$ ligand, trans to the $S3_{thiolate}$ atom. The Os−$S4_{thioether}$ distance [2.4035(15) Å], trans to a PMe_2Ph ligand, is longer than the mutually trans Os−$S3_{thiolate}$ and Os−$S5_{thiolate}$

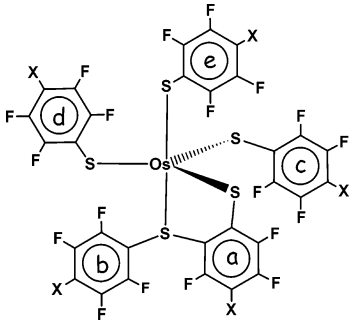

Figure 5. Drawing of **1** (X = F) or **2** (X = H) showing the different phenyl rings. Although the NMR absorptions are linked to the aromatic rings **a**−**e**, except for the rigid ring **a**, no definitive **b**−**e** correspondence can be established.

distances [2.3247(16) and 2.3659(16) Å, respectively], which reflects the greater trans influence of the phosphine ligands compared to the thiolate ligands. These $Os-S_{thiolate}$ distances are similar to those, also mutually arranged trans, in the related osmium(III) complex $[Os(SC_6F_4H\text{-}4)_2(S_2CSC_6F_4H\text{-}4)(PMe_2Ph)_2]$[39] [2.3459(14) and 2.3476(14) Å]. In **3**, both Os−P bond lengths are similar [2.3559(17) and 2.3414(16) Å] and compare well with the corresponding Os−P distances in $[Os(SC_6F_4H\text{-}4)_2(S_2CSC_6F_4H\text{-}4)(PMe_2Ph)_2]$[39] [2.3706(13) and 2.3422(13) Å].

The molecular structure of **4** shows an essentially trigonal-bipyramidal coordination geometry with an axial PPh_3 ligand and two equatorial $SC_6F_4H^-$ groups. The chelating thiolate−phenoxide ligand, *o*-$OSC_6F_3H^{2-}$, occupies both remaining axial (through O20) and equatorial (through S1) positions. Hence, the ligand *o*-$OSC_6F_3H^{2-}$ forms a five-membered chelate ring with the osmium atom, and the plane defined by the Os/S1/O20/C_6F_3H group is a bisector of the S2−Os−S3 angle, minimizing sterical hindrance in the molecule. The structure of **4** resembles that of $[Os(SC_6F_5)_2(o\text{-}S_2C_6F_4)(PMe_2Ph)]$.[33] There are no significant differences in equatorial distances $Os-S_{thiolate}$ between these two compounds. However, the Os−P distance in **4**, 2.3333(12) Å, is shorter than the corresponding distance in $[Os(SC_6F_5)_2(o\text{-}S_2C_6F_4)(PMe_2Ph)]$,[33] 2.374(4) Å, which reflects the larger trans influence of a thiolate ligand compared with a phenoxide ligand.

For both Os−O bonds trans to phosphine in complex **3**, $Os^{III}-O_{phenoxide}$, and complex **4**, $Os^{IV}-O_{phenoxide}$, the bond lenghts are similar, a fact that has been attributed to a compensating balance between electrostatic attraction and effective covalent bonding.

The perfluorinated compound **1** was analyzed in solution by ^{19}F NMR spectroscopy. If the C_6F_5 rings are not restricted to rotate about their C−S bonds and assuming that the solid-

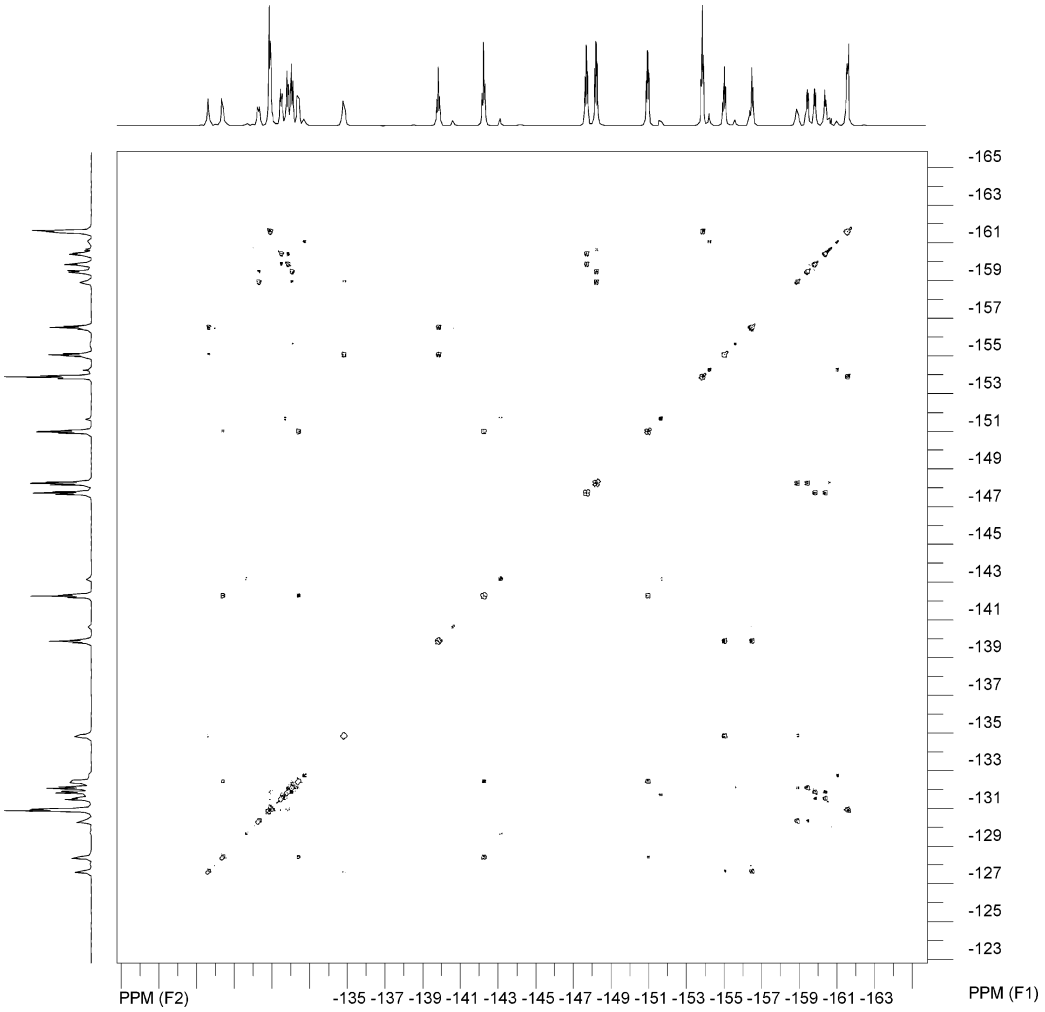

Figure 6. COSY $^{19}F-^{19}F$ NMR spectrum of **1** at −50 °C.

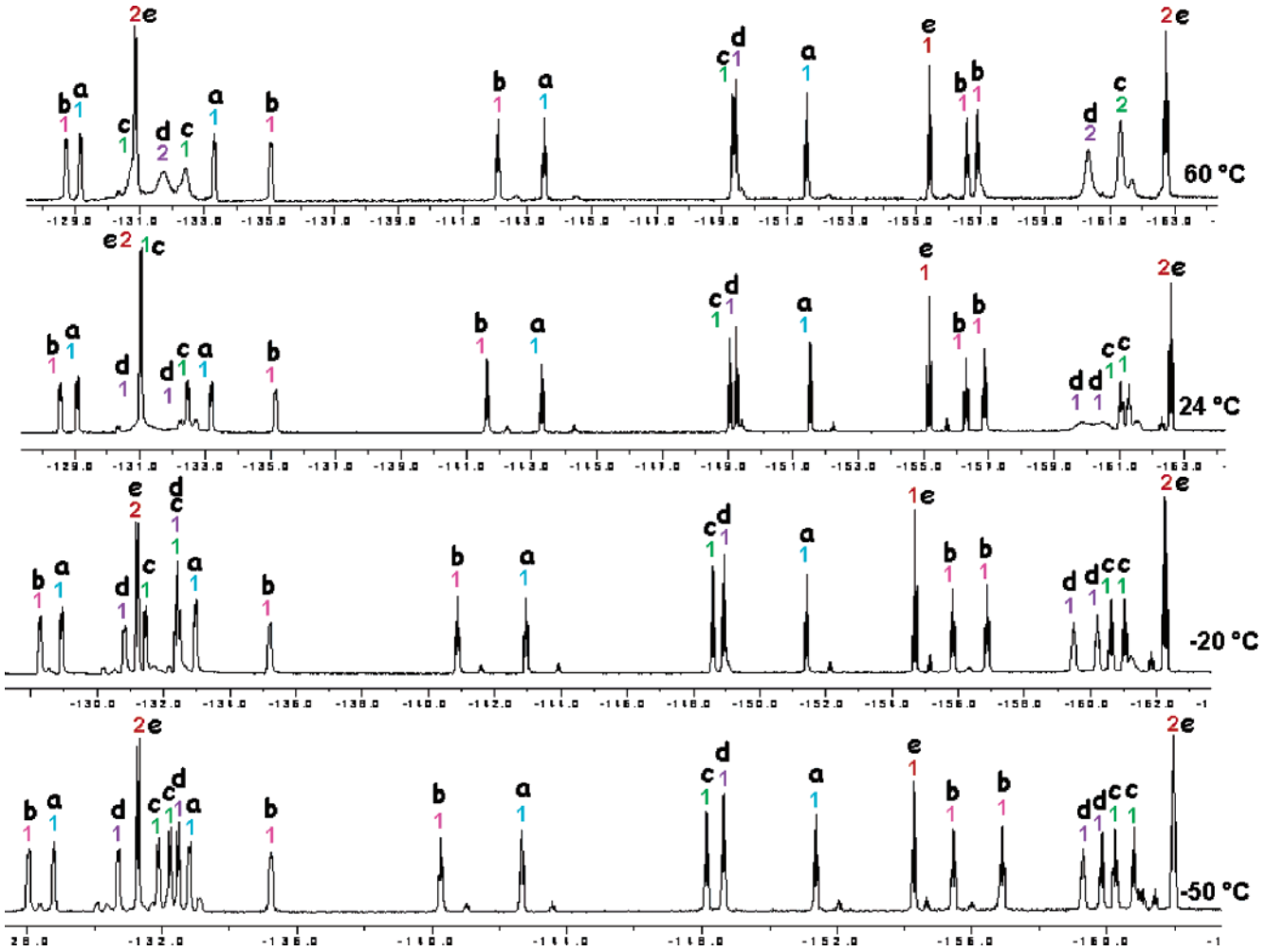

Figure 7. ^{19}F NMR spectra of **1** at −50, −20, +24, and +60 °C. The letter labels identify the signals that correspond to the same fluorinated ring, including the relative integrals.

state structure of **1** is retained in solution, one would expect a 16-absorption spectrum: four groups of three different resonances for the *o*-, *p*-, and *m*-fluorine atoms, at low, medium, and high fields, respectively (relative intensities in each group: 2:1:2),[40] corresponding to four distinct C_6F_5 fragments, and a further group of four different absorptions (intensities 1:1:1:1) for the C_6F_4 group. In contrast, the ^{19}F NMR spectra at room temperature exhibit 19 signals. When the ^{19}F NMR spectra were recorded at −50 °C, 22 different resonances were found, 2 of them with relative integrals of 2 and the other 20 with relative integrals of 1, giving a total of 24 fluorine atoms as in the X-ray diffraction structure (Figures 1 and 5). The COSY $^{19}F-^{19}F$ NMR spectrum at −50 °C confirms five subspectra corresponding to four C_6F_5 and one C_6F_4 groups (Figure 6). Three of the C_6F_5 subspectra correspond to AA′BCC′ spin systems (intensities 1:1:1:1:1), one corresponds to an A_2BC_2 spin system (intensities 2:1:2), and the C_6F_4 subspectrum exhibits an ABCD spin pattern (intensities 1:1:1:1). This spectrum at −50 °C is consistent with three C_6F_5 rings subject to restricted rotations about their C−S bonds, one C_6F_5 ring with free C−S bond rotation, and the additional rigid C_6F_4 ring, consistent with its chelating character.

The ^{19}F NMR spectra were measured every 10 or 5 °C, from −80 to +80 °C, whereas COSY $^{19}F-^{19}F$ NMR spectra were determined at −50, −20, 24, and 60 °C in order to follow the evolution and confirm the assignation of the absorptions corresponding to each subspectrum. Figure 7 shows the corresponding one-dimensional spectra at these temperatures, including their relative integrals.

The spectra at high temperature (ca. 80 °C) are consistent with the presence of three C_6F_5 groups (**c**, **d**, and **e**) with free C−S bond rotation. As the temperature is lowered, the signals ortho (2) and meta (2) from the **c**-C_6F_5 group collapse, each one giving rise to a pair of signals (1:1 and 1:1) that reach their maximum definition at ca. −50 °C. In sequence, two more absorptions, ortho (2) and meta (2) from the **d**-C_6F_5 group, follow a similar behavior and collapse as the temperature is decreased, suggesting that the **c**-C_6F_5 group finds an increased restriction to rotate around its C−S bond. The **b**-C_6F_5 group is also restricted to rotate, in this case within the full range of registered temperatures (always 1:1:1:1:1), being the most restricted C_6F_5 group to rotate. A fourth group of C_6F_5 signals (**e**) remains unchanged (systematically 2:1:2), suggesting that this group shows no restrictions to undergo C−S bond rotation along the full

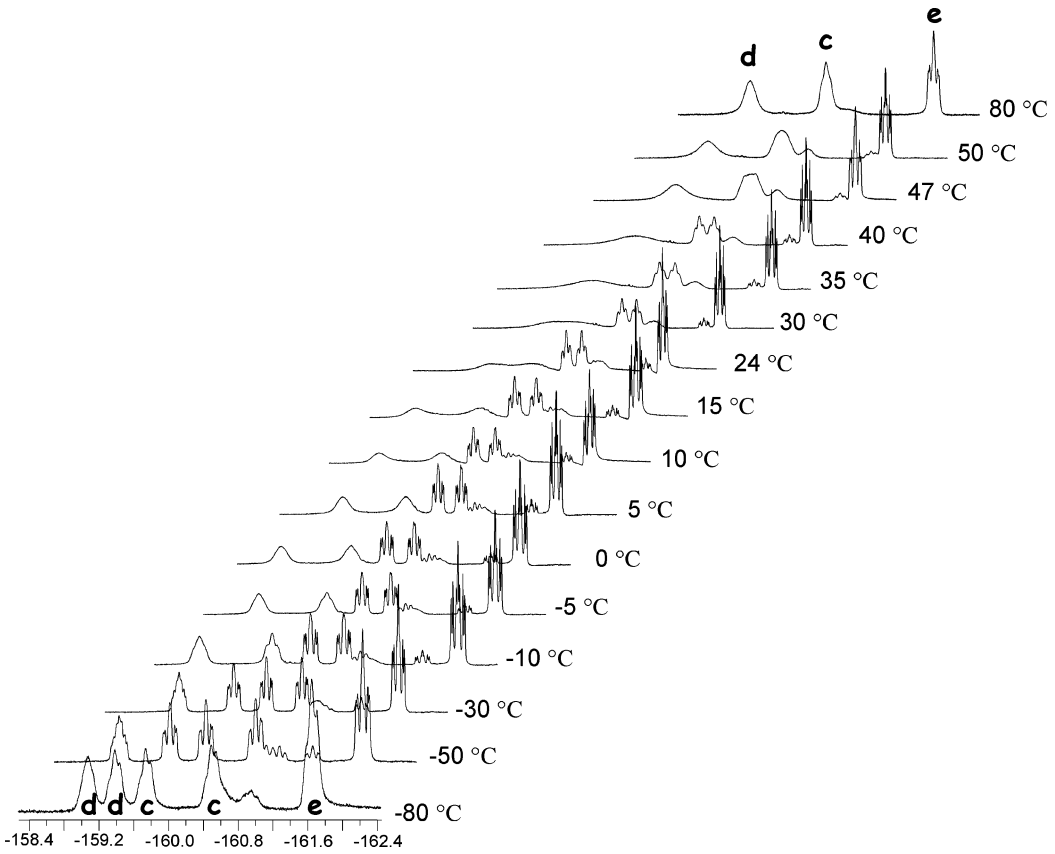

Figure 8. VT ^{19}F NMR spectra of **1** on the meta region of the **c**−**e** groups.

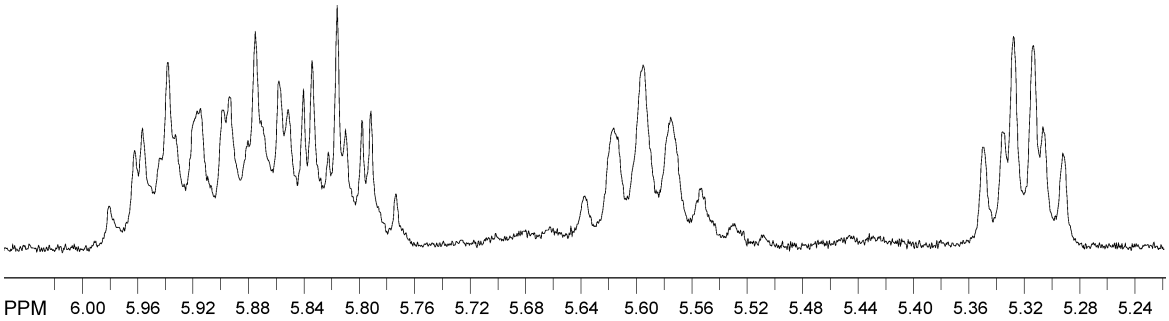

Figure 9. Room-temperature ^{1}H NMR spectrum of **2**.

range of studied temperatures. For obvious reasons, the C_6F_4 ring (**a**) of the chelating ligand is always impeded to rotate (always 1:1:1:1).

From detailed analyses of the VT ^{19}F NMR spectra in the region of meta absorptions (Figure 8), the free energies of activation for C−S bond rotation of both C_6F_5 groups (**c** and **d**) have been calculated as $\Delta G^{\ddagger} = 62 \pm 2$ kJ·mol^{-1} for the group **c** (coalescence temperature = 47 °C) and $\Delta G^{\ddagger} = 58 \pm 2$ kJ·mol^{-1} for the group **d** (coalescence temperature = 30 °C).

Room-temperature ^{1}H NMR spectra of compound **2** (Figure 9) show, in the aromatic region, five equally intense resonances corresponding to the five nonequivalent hydrogen atoms as found in the solid-state structure (Figures 2 and 5): four signals, triplet of triplets, attributed to the para hydrogens of four nonequivalent C_6F_4H-4 rings and, at higher field, one multiplet corresponding to the C_6F_3H ring.

2 affords a set of ^{19}F and COSY ^{19}F−^{19}F NMR spectra equivalent to that discussed above for compound **1**. VT ^{19}F NMR experiments also show that compounds **1** and **2** share a similar fluxional behavior. For compound **2**, from analyses of the VT ^{19}F NMR data in the region of meta absoptions, we have calculated the free energy of activation for the C−S bond rotation process in the corresponding **d** group as $\Delta G^{\ddagger} = 59 \pm 2$ kJ·mol^{-1} (coalescence temperature = 45 °C). However, some overlap of signals precludes the corresponding calculation for the **c** group.

It is important to notice that NMR spectroscopy is unable to distinguish between each of the fluorinated aryl substit-

(37) Matsukawa, S.; Kuwata, S.; Hidai, M. *Inorg. Chem. Commun.* **1998**, *1*, 368−371.
(38) Rossi, A. R.; Hoffmann, R. *Inorg. Chem.* **1975**, *14*, 365−374.
(39) Arroyo, M.; Bernès, S.; Cerón, J.; Rius, J.; Torrens, H. *Inorg. Chem.* **2004**, *43*, 986−992.
(40) Bertrán, A.; García, J.; Martin, E.; Sosa, P.; Torrens, H. *Rev. Soc. Quím. Méx.* **1993**, *37* (4), 185−191; *Chem. Abstr.* **1993**, *122*, 329084j.

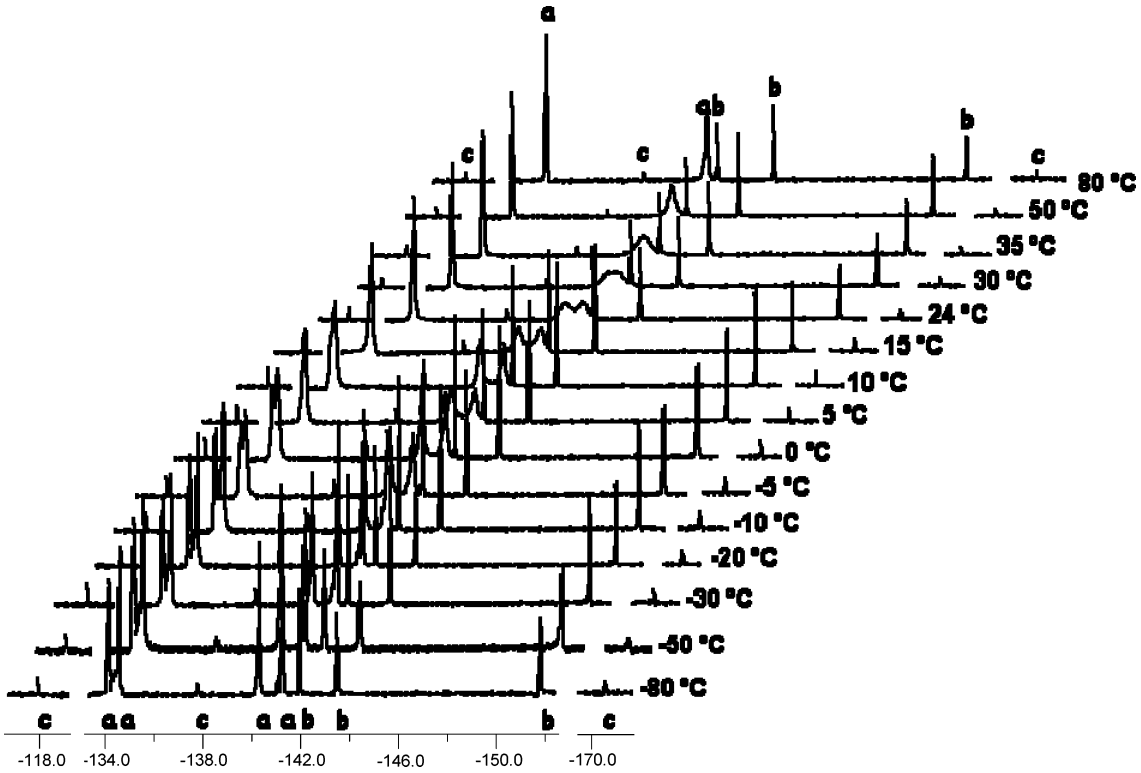

Figure 10. VT ^{19}F NMR of **4**: signals **a** from SC_6F_4H (both isomers), signals **b** from *o*-OSC_6F_3H (isomer A), and signals **c** from *o*-OSC_6F_3H (isomer B).

uents in each of the compounds **1** and **2** except when they are part of a rigid chelating ligand as found in ($SC_6\mathbf{F_4}(SC_6F_5)$-2), compound **1**, and ($SC_6\mathbf{F_3}H$-4-(SC_6F_4H-4)-2), compound **2**. Therefore, the NMR absorptions are linked to aromatic rings **a**, **b**, **c**, **d**, and **e** on each compound but, except for the rigid rings **a**, no definitive assignment can be done.

VT ^{19}F NMR spectra of compound **4** show this molecule to be also fluxional. At high temperature (ca. 80 °C), the ^{19}F NMR spectra of compound **4** (Figure 10) exhibit two signals (**a**; A_2B_2 spin system, intensities 4.4:4.4) corresponding to the *o*- and *m*-fluorine nuclei of two magnetically equivalent $(SC_6F_4H\text{-}4)^-$ ligands and three additional absorptions (**b**; intensities 1:1:1) arising from each of the three fluorine nuclei at the $(OSC_6F_3H)^{2-}$ moiety (ABC spin system). As the temperature is lowered, the meta signal from the SC_6F_4H-4 groups broadens, decreases in height, and eventually collapses (below 30 °C), giving rise to a pair of signals with the same intensity. This pair reaches its full definition at ca. −50 °C without further changes. The ortho signal from these SC_6F_4H-4 groups remains as a single band until ca. 10 °C, although its relative height began to decrease from ca. 50 °C and, at ca. 5 °C, also collapses, giving rise to a pair of signals with the same intensity (the scale in Figure 10 does not allow one to appreciate this collapse at 5 °C, but the corresponding expansions does allow it). This pair also reaches its maximum definition at ca. −50 °C without further changes. The different coalescence points of the ortho (10 °C) and meta (30 °C) signals from the SC_6F_4H groups of **4** are explained considering the different proximity of the chemical shifts between both ortho or both meta signals. However, as expected, free energies of activation $\Delta G^{\ddagger}$ calculated from ortho and meta parameters result in practically equal values within experimental error (below). Except for small variations due to subtle changes in the magnetic couplings, the subspectra arising from the thiolate−phenoxide fragment remain essentially unchanged through the full range of temperatures. An additional subspectrum (**c** signals; ABC spin system, intensities 0.1:0.1:0.1), which also remains unchanged along the full range of temperatures, suggests that **4** exists as the pair of structural isomers shown as follows:

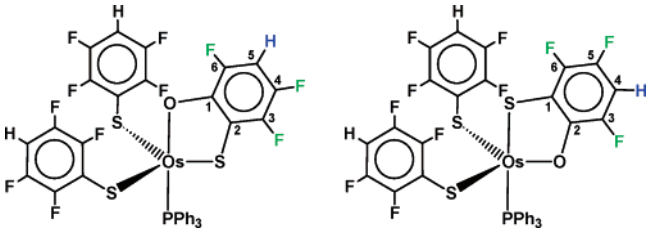

Both isomers differ in the relative position of the hydrogen atom at the thiolate−phenoxide ring either attached to carbon-5 or carbon-4 relative to the axial oxygen or sulfur atom. ^{19}F NMR spectra indicate that both isomers are present in relative amounts of ca. 10:1. Two-dimensional ^{19}F−^{19}F NMR experiments confirmed two subspectra for the SC_6F_4H and OSC_6F_3H groups of the more abundant isomer.

The ^{31}P{^{1}H} NMR spectra of **4** exhibit two singlets with relative integrals of ca. 10:1 corresponding to each one of the isomers.

^{1}H NMR spectra of **4** are also consistent with the presence of these two isomers in a ratio of ca. 10:1. Thus, in addition to the signals corresponding to the protons of the C_6H_5 rings from the PPh_3 axial ligand, and only one signal of the SC_6F_4H

groups for both isomers, two signals attributed to the *o*-OSC_6F_3H fragment of each one of the isomers with relative integrals of ca. 10:1 are also present. Thus, it is evident from the ^1H and ^{19}F NMR spectra that the SC_6F_4H groups from isomers A and B are magnetically equivalent, while the corresponding OSC_6F_3H groups are not. The fluxional behavior of this compound can be attributed, as in the previous cases, to a hindered rotation around the $S-C_6F_4H$ bonds on this geometry. We have calculated the corresponding free energies of activation for **4** from the analyses of VT ^{19}F NMR spectra in the regions of both ortho and meta (SC_6F_4H-4) absorptions, resulting in practically the same values within experimental error, 55 ± 2 and 57 ± 2 kJ·mol^{-1}, respectively.

The formation of **1** and **2** from OsO_4 and HSC_6F_5 or HSC_6F_4H involves cleavage of an *o*-C−F bond at a SC_6F_5 or SC_6F_4H group, respectively. The mechanism of these reactions has still not been established, but because the products **1** and **2** bear $(SC_6F_4(SC_6F_5)\text{-}2)^-$ or $(SC_6F_3H\text{-}4\text{-}(SC_6F_4H\text{-}4)\text{-}2)^-$ ligands, respectively, one of the original SR moieties had to be involved in a reaction such that an *o*-fluorine atom is replaced by a sulfur atom.

On the other hand, the formation of **3** from $[Os(SC_6F_5)_3(PMe_2Ph)_2]$ or $[Os(SC_6F_5)_4(PMe_2Ph)]$ and KOH involves two ruptures of *o*-C−F bonds at SC_6F_5 groups, whereas an *o*-fluorine atom is replaced by oxygen, with the formation of new C−O and Os−O bonds. The formation of **4** from $[Os(SC_6F_4H\text{-}4)_4(PPh_3)]$ and KOH implies the cleavage of an *o*-C−F bond at a SC_6F_4H group and its simultaneous replacement by an oxygen atom with the formation of a thiolate−phenoxide ligand. Nucleophilic displacement of *o*-fluorine by OH^- from a C_6F_5 ring bound to phosphorus had previously been observed in the formation of *trans*-$[Pt(CH_3)(o\text{-}OC_6F_4PPh_2)(PPh_2(C_6F_5))]$,[41,42] prepared from *trans*-$[Pt(CH_3)(THF)(PPh_2(C_6F_5))_2]$ and KOH.

The free energies of activation for the rotations about the $S-C_6F_5$ or $S-C_6F_4H$ bonds, calculated to be 62 ± 2 kJ·mol^{-1} (group **c**) and 58 ± 2 kJ·mol^{-1} (group **d**) [compound **1**], 59 ± 2 kJ·mol^{-1} (group **d**) [compound **2**], and 56 ± 3 kJ·mol^{-1} [compound **4**], are close to the corresponding free energies of activation in $[Os(SC_6F_5)_2(o\text{-}S_2C_6F_4)(PMe_2Ph)]$[33] and $[Os(SC_6F_4H)_2(o\text{-}S_2C_6F_3H)(PMe_2Ph)]$[33] ($59 \pm 4$ kJ·mol^{-1}) and are also close to those found for $P-C_6F_5$ bond rotations (55 ± 2 kJ·mol^{-1}).[43]

Acknowledgment. We are grateful to CONACYT (Grant 27915E) and VIEP (Grant 03/NAT/06-G) for financial support. S.B. acknowledges BUAP for the use of diffraction facilities.

Supporting Information Available: X-ray crystallographic files, in CIF format, for structures **1**−**4**. This material is available free of charge via the Internet at http://pubs.acs.org.

IC0619660

(41) Park, S.; Pontier-Johnson, M.; Roundhill, D. M. *Inorg. Chem.* **1990**, *29*, 2689−2697.
(42) Park, S.; Pontier-Johnson, M.; Roundhill, D. M. *J. Am. Chem. Soc.* **1989**, *111*, 3101−3103.
(43) Atherton, M. J.; Fawcett, J.; Holloway, J. H.; Hope, E. G.; Karaçar, A.; Russell, D. R.; Saunders, G. C. *J. Chem. Soc., Dalton Trans.* **1996**, 3215−3220.